ACS APPLIED MATERIALS & INTERFACES

Research Article

www.acsami.org

Uniform Dispersion of Lanthanum Hexaboride Nanoparticles in a Silica Thin Film: Synthesis and Optical Properties

Fei Jiang,*[,†,‡] Yee-Kwong Leong,[‡] Martine Saunders,[§] Mariusz Martyniuk,[†] Lorenzo Faraone,[†] Adrian Keating,[‡] and John M. Dell[†]

[†]School of Electrical, Electronic and Computer Engineering, University of Western Australia, Australia

[‡]School of Mechanical and Chemical Engineering, University of Western Australia, Australia

[§]Centre for Microscopy, Characterisation and Analysis, University of Western Australia, Crawley, WA, 6009, Australia

ABSTRACT: Silica thin films containing uniformly dispersed lanthanum hexaboride (LaB_6) nanoparticles have been prepared by spin-coating a sol–gel silica solution containing cetyltrimethyl ammonium bromide (CTAB)-stabilized LaB_6 nanoparticles onto a glass substrate followed by a standard heat treatment. The production of this thin film involved three steps: (i) a CTAB-stabilized LaB_6 nanoparticle dispersion was prepared in water and then dried, (ii) the dried nanoparticles were redispersed in a small amount of water and mixed with tetraethoxyorthosilane (TEOS), ethanol, and a little acid to initiate the sol–gel reaction, and (iii) this reaction mixture was spun to produce a thin film and then was annealed. A range of techniques such as zeta potential, laser sizing, energy-filtered transmission electron microscopy (EFTEM), scanning TEM (STEM), scanning electron microscopy (SEM), and energy dispersive X-ray spectrum (EDS) were employed to characterize the particle's size, elemental composition, and stability and the optical properties of silica thin films with LaB_6 nanoparticles. On the basis of the optical transmittance and reflectance spectra of an annealed silica thin film with LaB_6 nanoparticles, the annealed thin films clearly showed positive absorption of radiation in the near infrared (NIR) region meeting a main objective of this study. A potential optical micro-electromechanical sensing system in the NIR range can be realized on the basis of this silica thin film with LaB_6 nanoparticles.

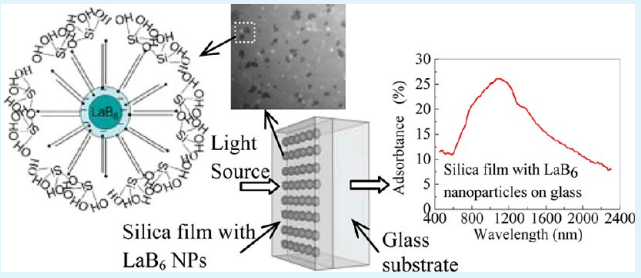

KEYWORDS: *LaB_6 nanoparticles, silica thin film, surface plasmon resonance, NIR absorption, surfactant stabilization*

1. INTRODUCTION

LaB_6 nanoparticles with size less than ~120 nm exhibit excellent light absorbing properties in the near infrared (NIR) region extending from 650 to 1600 nm[1,2] due to surface plasmon resonance effects and are used commercially to reduce heat transmission through laminated windows and car windscreens.[3,4] This technology is based on dispersal of the nanoparticles in an organic material used for the lamination process and has been described by Takeda et al.[2] The preparation of LaB_6 nanoparticles in an aqueous medium as one of the feed materials to produce a silica thin film containing uniformly dispersed un-agglomerated LaB_6 nanoparticles has not been reported. Using a silica film as the host matrix allows the film to be subjected to standard semiconductor and micro-electromechanical systems (MEMS) processing, potentially expanding the application of LaB_6 nanoparticles to MEMS for microelectronics,[5] sensors,[6] or optical coatings.[7] To achieve high NIR absorbance, it requires dispersal of the LaB_6 nanoparticles uniformly in a matrix while still meeting several key requirements including material uniformity, small size, narrow size distribution, and sufficiently high concentration of nanoparticles, which has been a challenge to date if the host matrix is inorganic.

There have been two main approaches used to fabricate thin films containing dispersed nanoparticles.[8−11] The first method is to graft organic passivating ligands onto the nanoparticles so that they can be dispersed in an organic solvent prior to generating a thin film by coating/casting and drying.[2] The difficulty with this approach is that the nanoparticles are hydrophobic and can only be dispersed in some organic solvents.[12] In addition, nanoparticles are aggregated by the van der Waals interactions between grafted alkyl chains surrounding each particle. This has the potential to weaken the chemical and thermal stability of the nanoparticle coated by polymer under the high temperature and acid condition because of low intrinsic stability of polymers.[10,12] The second method is applicable to the dispersion of nanoparticles in a hydrophilic thin film matrix made from materials such as silica or titania and is based on a surfactant stabilization of nanoparticles to allow dispersion in water.[10,13−18] The surfactant stabilization approach possesses several advantages including excellent reproducibility in processing uniformly dispersed nanocrystals

Received: July 27, 2012
Accepted: October 11, 2012
Published: October 11, 2012

in the thin film with an adjustable nanocrystal concentration. This approach has been used to disperse various kinds of nanoparticles in sol−gel silica solution, including gold[10] and Ln-doped LaF.[11] The use of this technique has not been demonstrated for LaB_6 nanoparticles.

Herein, we report (i) the production of water-dispersed LaB_6 nanoparticles and (ii) an approach to produce uniformly dispersed LaB_6 nanoparticles in a silica thin film via the sol−gel process.[19] A cetyltrimethyl ammonium bromide (CTAB) surfactant is used to stabilize and reduce the agglomeration of the LaB_6 nanoparticles in water. As delivered, the untreated LaB_6 particles had an apparent size of ∼700 nm when dispersed in water after ultrasonication, compared to ∼120 nm for the CTAB-stabilized LaB_6 nanoparticles. Zeta potential[20] and particle size characterization were used to determine the stability of the LaB_6 nanoparticles in water and CTAB solution. In addition, silica films containing LaB_6 nanoparticles have been demonstrated. Scanning electron microscopy (SEM) and transmission electron microscopy (TEM) were used to verify the function of the surfactant and the dispersion of the LaB_6 nanoparticles in silica film. Optical spectroscopy was used to measure the transmission, reflectance, and absorption properties of the LaB_6 nanoparticles/silica thin film on a glass substrate. A 10% transmission change is measured using a 1 μm thick silica film containing 0.27 wt % LaB_6 nanoparticles spun coated onto a glass substrate.

2. MATERIALS AND EXPERIMENTAL METHODS

The LaB_6 nanoparticles used in this work were purchased from MIT Corp. The other chemicals used were analytical reagent grade: NaOH (AR), CTAB (99.0%), tetraethoxyorthosilane (TEOS, 99.0%), ethanol (AR, 99.5%), and HCl (AR, 37wt.%). All items were purchased from Sigma-Aldrich.

In the preparation of the water-dispersed CTAB-stabilized LaB_6 nanoparticles, 20 mg of LaB_6 nanoparticles was added to 20 mL of water at pH 11, with the pH adjusted by the addition of NaOH. The mixture was then sonicated with a Vibra Cell VCX 500 1/2 inch sonic probe for 1 min. Then, CTAB (50 mg) was slowly added to the LaB_6 nanoparticle aqueous suspension over a period of 3 min while undergoing vigorous ultrasonication to minimize particle agglomeration. The aqueous suspension of the dispersed CTAB-stabilized LaB_6 nanoparticles was left to settle for 14 days. The procedure of fabrication has been shown in Scheme 1. This CTAB-stabilized fabrication process was repeated several times and achieved the same results.

Scheme 1. CTAB-Stabilized LaB_6 Nanoparticle Fabrication Procedure

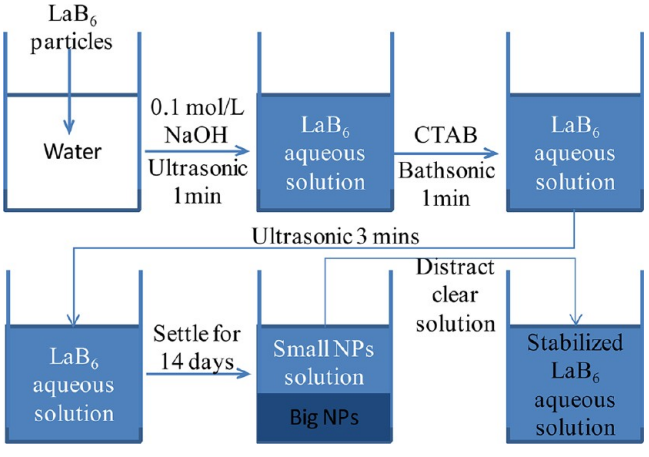

CTAB-stabilized LaB_6 nanoparticles were collected from the aqueous suspension by centrifuging at 10 000 rpm for 20 min. After drying, the CTAB-stabilized nanoparticles could be easily redispersed in water, exhibiting an average size of 120 nm at pH 11 as measured using dynamic light scattering (DLS)[20] in a Malvern Nano Zetasizer. The size distribution and zeta potential of untreated LaB_6 and CTAB-stabilized LaB_6 particles in water are shown in Figure 1.

The sol−gel material used to form the spin coated LaB_6 nanoparticle/silica thin film was prepared by dispersing 1.5 mg of CTAB-stabilized LaB_6 nanoparticles in 0.4 mL of water and then mixing with 2 mL of TEOS and 2.2 mL of ethanol. The pH of the mixed solution was adjusted to 2 by addition of 0.1 N HCl and then stirred for 24 h. The resulting sol−gel silica solution containing the dispersed LaB_6 nanoparticles was spun onto a glass substrate at 1000 rpm/40 s and heated to 400 °C for an hour.

The zeta potential and particle size distribution in the aqueous suspensions of untreated LaB_6 nanoparticles and CTAB-stabilized LaB_6 nanoparticles were measured using a Malvern Nano Zetasizer. In this measurement, HCl and NaOH were added to the LaB_6 aqueous suspensions to examine the effect of varying pH on dispersal and agglomeration.

Particle size and morphology were investigated by secondary electron imaging with a Zeiss 1555 variable pressure SEM using two samples, prepared by the aqueous suspensions containing untreated LaB_6 nanoparticles and CTAB-stabilized LaB_6 nanoparticles, respectively. In the sample preparation, a couple of drops of each solution were dropped onto an Al SEM stage and then put under an infrared lamp for 3−5 min to dry. All samples were then coated with ∼10 nm of carbon prior to imaging.

TEM imaging, scanning TEM (STEM) imaging, and microanalysis were also used to characterize the compounds present in the dried CTAB-stabilized LaB_6 nanoparticles and the silica thin film containing LaB_6 nanoparticles. A JEOL 3000F field emission TEM operating at 300 kV and equipped with a Gatan Orius SC1000 CCD camera, Gatan Imaging Filter (GIF), and Oxford Instruments INCA energy dispersive X-ray spectrum (EDS) system was used for all TEM analyses. Element mapping was carried out with the GIF by energy-filtered TEM (EFTEM) using the conventional three-window technique.[21] For preparation of EFTEM samples, a drop of the solution containing the dispersed CTAB-stabilized nanoparticles was placed on a copper mesh TEM grid coated with continuous carbon support film and then dried under an infrared lamp. For the STEM and EDS measurements, a sol−gel silica suspension with uniformly dispersed LaB_6 nanoparticles will be spun to produce a silica thin film on a continuous carbon-coated Cu TEM grid. First, the grid will be stuck on a silicon substrate using crystal wax. Then, the silica solution with nanoparticles was spun onto the silicon substrate. Taking into consideration the thickness required for STEM imaging, a spinning speed of 5000 rpm/40 s was employed to produce a ∼250 nm thick film. After spinning, the sample was heated for 30 min at 200 °C.

Optical spectroscopy was used to measure the transmission and reflectance of a silica thin film with dispersed CTAB-stabilized LaB_6 nanoparticles on a glass substrate. The thickness of this thin film was ∼1 μm. The transmittance and reflectance were subsequently used to calculate the absorbance of the LaB_6 NPs/silica thin film. To acquire high intensity of LaB_6 nanoparticles in silica film, a 1000 rpm/40 s spinning procedure was used to form a thick film. After the spinning process, the sample was annealed for an hour at 400 °C in an air atmosphere.

3. RESULTS AND DISCUSSION

The relationship between average particle size and zeta potential of the untreated LaB_6 nanoparticle aqueous suspensions and CTAB-stabilized LaB_6 nanoparticle aqueous suspensions at various pH levels is shown in Figure 2. In the absence of CTAB, agglomeration of the unstabilized LaB_6 is evident as shown in Figure 2a. The measured average particle size is large, ranging from 700 to 1200 nm. The primary size of these particles, according to the nanoparticle's supplier, should

dx.doi.org/10.1021/am301481j | ACS Appl. Mater. Interfaces 2012, 4, 5833−5838

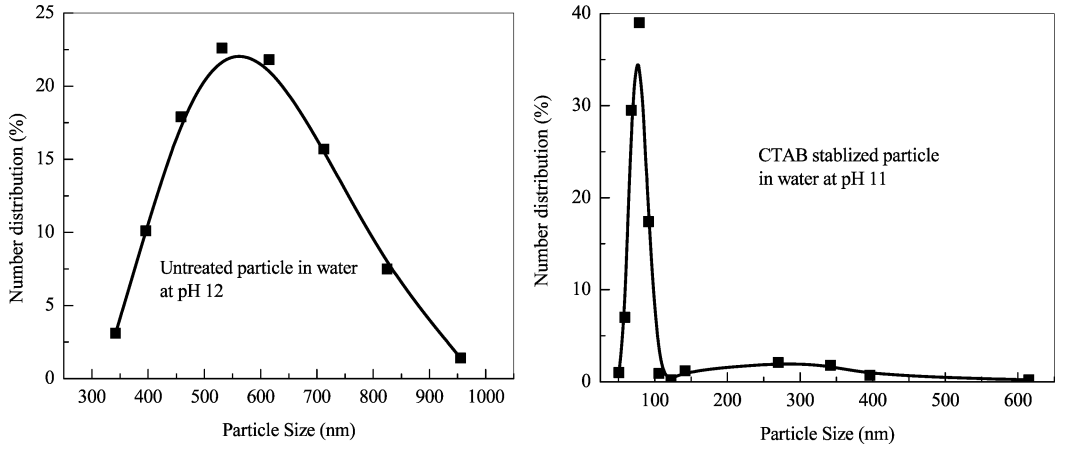

Figure 1. Size distribution of untreated LaB_6 and CTAB stabilized LaB_6 nanoparticles.

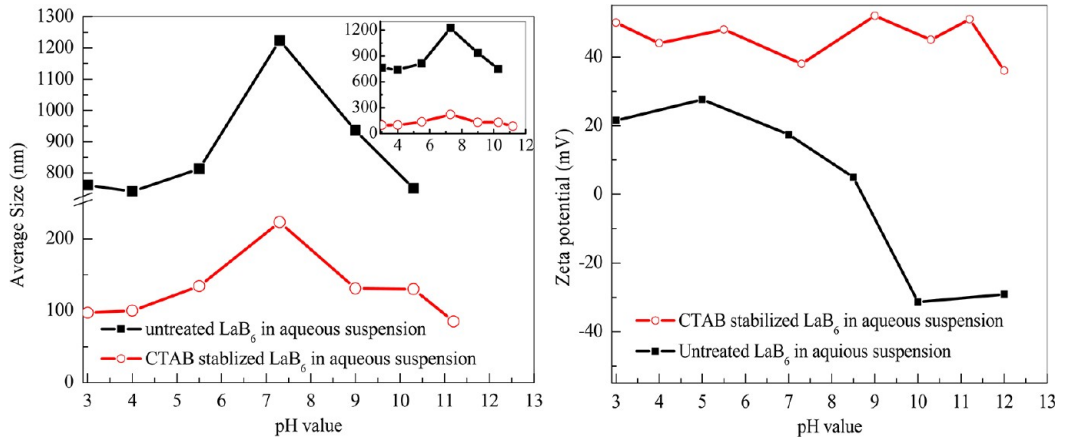

Figure 2. Zeta potential and average size of untreated LaB_6 nanoparticles and CTAB-stabilized LaB_6 nanoparticles in aqueous solution as a function of pH value.

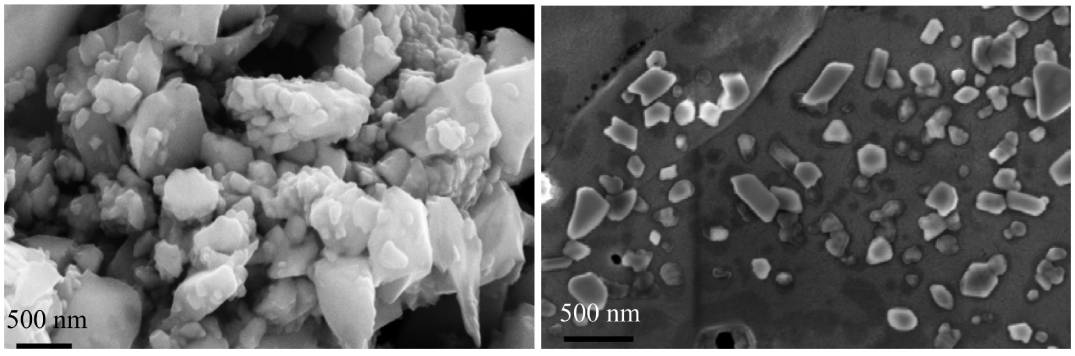

Figure 3. Secondary electron SEM images of dried untreated LaB_6 nanoparticles (left) and CTAB-stabilized LaB_6 nanoparticles (right) from water.

be nominally 55 nm. The size variation with pH was, however, very different for CTAB-stabilized LaB6 nanoparticles. The average size is much smaller. It fell predominantly within a narrow range between 75 and 100 nm over the pH range of 3−11.5. However, one average size value was 250 nm located at pH 7.5.

The zeta potential of untreated LaB_6 nanoparticles and CTAB-stabilized LaB_6 nanoparticles were also measured. The results are shown in Figure 2b. For the untreated LaB_6 nanoparticles in aqueous suspension, the particles are negatively charged with a zeta potential of ∼−30 mV at pH 10 and positively charged at pH 5 with the same magnitude of zeta potential. In contrast, the zeta potential of CTAB-stabilized LaB_6 nanoparticles remained essentially constant and positive. It spanned between 37 and 50 mV over the whole pH range of 3−12.

The results in Figure 2 showed a clear correlation between the average size and zeta potential of particles. For unstabilized LaB_6 nanoparticles in aqueous suspension, the maximum particle size of 1200 nm appeared to be located at the point of zero charge or the isoelectric point (IEP) of the particle in water at pH 8.8. A strong agglomeration of the primary particles leading to a larger size is expected at this point as the van der Waals attractive force strongly dominates the particle

dx.doi.org/10.1021/am301481j | ACS Appl. Mater. Interfaces 2012, 4, 5833−5838

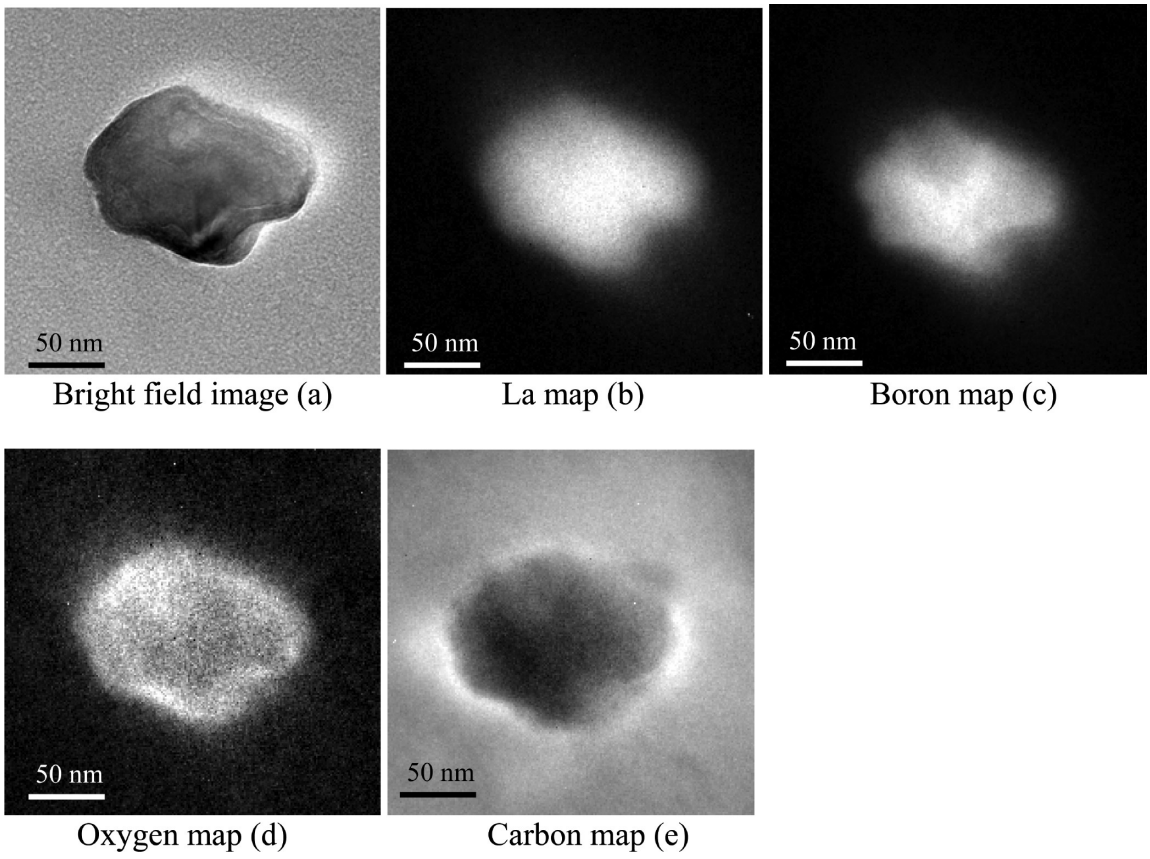

Figure 4. EFTEM for CTAB-stabilized LaB_6 nanoparticles.

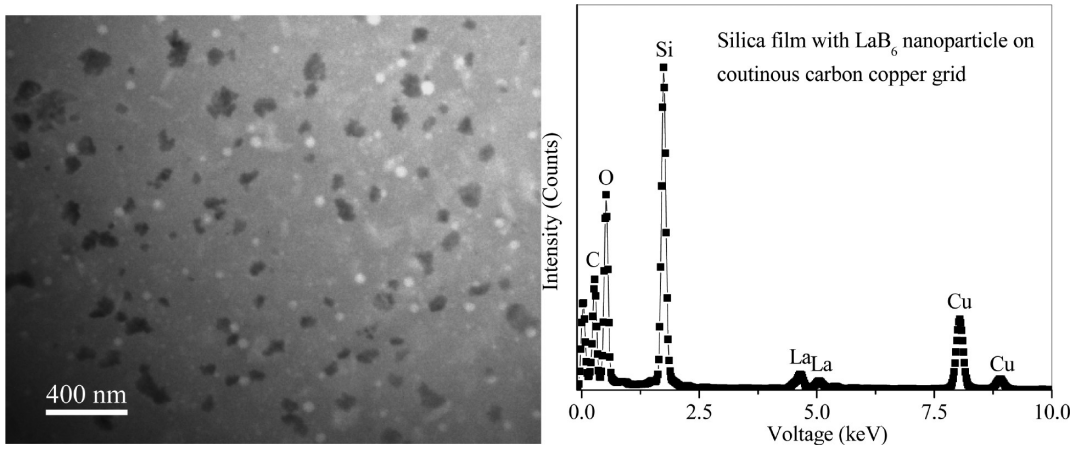

Figure 5. (a) STEM image of CTAB-stabilized LaB_6 nanoparticles in silica film and (b) the corresponding energy dispersive spectrum (EDS). (The bright regions in the STEM image are voids or holes in the silica film.)

interactions while repulsive force is very weak or nonexistent. In contrast, CTAB-stabilized LaB_6 nanoparticles are covered by the positively charged CTAB molecules resulting in higher zeta potentials that supply larger repulsive forces to counteract the van der Waals force. This high zeta potential result also provides direct evidence that CTAB has been adsorbed onto the LaB_6 particles. In addition, the adsorbed CTAB layer also acts as a steric layer,[22] resulting in electrosteric stabilization.[22]

It should be noted that CTAB is a quaternary amine compound with a single permanent positive charge. For LaB_6 to be positive at a pH above its IEP, the amount of CTAB adsorbed must be more than the underlying negative surface charge of the LaB_6, requiring a combination of charged and hydrophobic adsorption of CTAB molecules onto LaB_6 surface. In this study, LaB_6−CTAB model structure is similar to that used by Fan et al. to describe their CTAB-stabilized gold particles.[10]

Figure 3 showed the SEM images of untreated LaB_6 nanoparticles (left) and CTAB-stabilized LaB_6 nanoparticles (right) after dispersal in water and then drying on an SEM mount, as described in the Materials and Experimental Methods section. It can be seen clearly that the untreated LaB_6 nanoparticles have agglomerated, while the CTAB-

dx.doi.org/10.1021/am301481j | ACS Appl. Mater. Interfaces 2012, 4, 5833−5838

stabilized LaB_6 nanoparticles are uniformly dispersed with little or no agglomeration.

Direct evidence of the presence of the adsorbed CTAB layer on the LaB_6 particle surface was obtained from elemental mapping, particularly of the carbon distribution, using EFTEM. Figure 4 shows a series of EFTEM element maps of CTAB-stabilized LaB_6 particles. Figure 4a shows the bright field TEM image of the particle with a CTAB layer. Figure 4b–e shows the lanthanum (La), boron (B), oxygen (O), and carbon (C) maps of the particles, respectively. The La and B mapping images indicate that the predominant surface of the particle is lanthanum boride. However, the La rich region is slightly larger than B mapping area, compared to Figure 4b,c. Additionally, a thin oxygen rich region is observed on the surface of lanthanum boride particle as shown in Figure 4d, which overlaps with the extension of the La region beyond the B region, indicating the presence of lanthanum oxide on the particle surface. A small degree of surface oxidation is unavoidable as these LaB_6 nanoparticles were kept in air. The carbon mapping result shown in Figure 4e indicates the presence of a carbon rich layer at the edge of the lanthanum rich region, as the carbon concentration is higher in this region than the background level from the carbon support film. Combining these results shown in Figure 2, the carbon rich layer is assumed to be indicative of the presence of CTAB on the particle surface. The EFTEM image showed the presence of oxygen on the surface of CTAB stabilized LaB_6 nanoparticles. The oxidized surface will also adsorb CTAB molecules as long as it is negatively charged.

To demonstrate the presence of uniformly dispersed LaB_6 nanoparticles in an inorganic thin film, dried CTAB-stabilized LaB_6 nanoparticles were used in the preparation of a thin silica film using a sol–gel and spin-coating process. Figure 5a shows a TEM image of the silica film containing the dispersed LaB_6 nanoparticles, with the corresponding energy dispersive X-ray spectrum (EDS) shown in Figure 5b. In Figure 5a, relatively uniformly dispersed LaB_6 nanoparticles (dark areas) can be clearly seen in the silica film. The particles showed a size distribution which is appropriately matched with the data from the Figure 2b. The bright regions in the STEM image are voids or holes in the silica film. For the TEM analysis, a thin film was spun directly onto the Cu TEM support grid. No postdeposition annealing is possible as the Cu grid is unstable at elevated temperature, which results in the voids/holes observed in Figure 5. An annealing step was, however, possibly undertook before the optical measurements (see below). Figure 5b shows the STEM EDS spectrum of LaB_6 nanoparticles in the silica film. The EDS spectrum confirmed the presence of La. Boron is too light to be detected with this technique, so the obvious La signal is taken to indicate the presence of LaB_6 nanoparticles in the film. The silicon and oxygen signals are expected to be from the silica film. The sample is mounted on a carbon-coated TEM grid, which results in additional carbon and copper peaks. The experimental result shown in Figure 5a appeared to support the model proposed by Fan et al.[10] in relation to the interaction between silacic acid and CTAB ligands. As can be seen from Figure 5a, the particles are not naturally spherical. Additionally, we have also measured the size distribution of these CTAB-stabilized LaB_6 nanoparticles with a Malvern Nanozeta sizer.

For optical characterization, a thicker silica film with a relatively high concentration of LaB_6 nanoparticles was prepared using the procedure given in the Materials and Experimental Methods section. To avoid the effect from the voids or holes on optical measurements, the samples of the silica films with and without LaB_6 nanoparticles on glass were annealed at 400 °C for an hour in an oven blanketed by an air atmosphere, before the optical transmittance and reflectance measurements. After annealing, the thickness of silica film containing LaB_6 nanoparticles was ~1 μm, and LaB_6 concentration was calculated to be 0.27 wt %. As shown in Figure 6, a pure silica reference film on glass shows a transmission change of ~5%, which might be caused by the constructive interference for light through a pure silica film or adsorption by the glass substrate. In addition, there is a 15% transmittance drop for a silica film with uniformly dispersed LaB_6 nanoparticles on a glass substrate. Therefore, the absorbance of NIR of 1050 nm wavelength is about 10%. This is considered a positive result although the amount absorbed is not as large as anticipated. The relatively low nanoparticle concentration, large size of LaB_6 nanoparticles, and the very thin silica film (~1 μm thick) hindering the loading of nanoparticles are believed to be responsible. The reflectance of LaB_6 nanoparticles and silica film with and without LaB_6 nanoparticles is around 4 % through the whole measured wavelength range. Actually, the apparent absorption at around 1050 nm in Figure 6 involves both absorption and scattering. However, the scattering contribution for the present size particles has been estimated as a small percentage through the whole measured range.

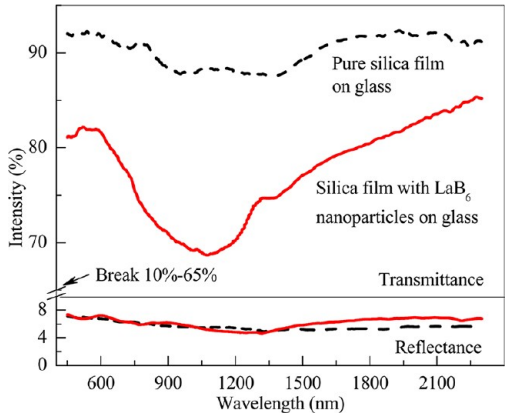

Figure 6. Transmittance and reflectance profiles of LaB_6 nanoparticles and LaB_6/silica film over the visible-near-infrared range.

4. CONCLUSION

To our knowledge, this is the first report of the preparation of uniformly dispersed CTAB-stabilized LaB_6 nanoparticles in a silica film with significant vis–NIR range absorbance properties. This work has demonstrated the synthesis of water-dispersed LaB_6 nanoparticles, a CTAB-stabilized LaB_6 nanoparticles/silica solution, and a silica film with uniformly dispersed LaB_6 nanoparticles. An adsorbed layer of CTAB on the LaB_6 nanoparticles has been confirmed by EFTEM characterization. The stabilization of the LaB_6 nanoparticles by a CTAB surfactant is attributed to an electrosteric mechanism. A NIR light absorbance silica film with uniformly dispersed LaB_6 nanoparticles has been successfully fabricated.

AUTHOR INFORMATION

Corresponding Author

*Tel.: +61-08-6488-3745. Fax: +61-08-6488-1095. E-mail: jiang@mech.uwa.edu.au.

Notes

The authors declare no competing financial interest.

ACKNOWLEDGMENTS

The work was supported by an Australian Research Council Discovery grant and an Australia-India Strategic Research Fund (AISRF) (ST030019). The authors also acknowledge the WA Node of the Australian National Fabrication Facility and the facilities and scientific and technical assistance of the Australia Microscopy & Microanalysis Research Facility at the Centre for Microscopy, Characterisation & Analysis, The University of Western Australia, a facility funded by the University, State and Commonwealth Governments. We wish to thank the reviewers' contribution for making this a better paper.

REFERENCES

(1) Schelm, S.; Smith, G. B.; Garrett, P. D.; Fisher, K. W. *J. Appl. Phys.* **2005**, *97*, 124314.
(2) Takeda, H.; Kuno, H.; Adachi, K. *J. Am. Ceram. Soc.* **2008**, *91*, 2897−2902.
(3) Smith, G. B.; Deller, C. A.; Swift, P. D; Gentle, A.; Garrett, P. D.; Fisher, W. K. *J. Nanopart. Res.* **2002**, *4*, 157−165.
(4) Schelm, S.; Smith, G. B. *Appl. Phys. Lett.* **2003**, *82*, 4346−4348.
(5) Maex, K.; Baklanov, M. R.; Shamiryan, D.; Iacopi, F.; Brongersma, S. H.; Yanovitskaya, Z. S. *J. Appl. Phys.* **2003**, *93*, 8793−8841.
(6) Melde, B.; Johnson, B.; Charles, P. *Sensors* **2008**, *8*, 5202−5228.
(7) Scott, B. J.; Wirnsberger, G.; Stucky, G. D. *Chem. Mater.* **2001**, *13*, 3140−3150.
(8) Jiang, C.; Singamaneni, S.; Merrick, E.; Tsukrui, V. V. *Nano Lett.* **2006**, 6.
(9) Godfrey Alig, A. R.; Akbulut, M.; Golan, Y.; Israelachvili, J. *Adv. Funct. Mater.* **2006**, *16*, 2127−2134.
(10) Fan, H.; Yang, K.; Boye, D. M.; Sigmon, T.; Malloy, K. J.; Xu, H.; Lopez, G. P.; Brinker, C. J. *Science* **2004**, *304*, 567−571.
(11) Sivakumar, S.; van Veggel, F. C. J. M.; Raudsepp, M. *J. Am. Chem. Soc.* **2005**, *127*, 12464−12465.
(12) Faraji, M.; Yamini, Y.; Rezaee, M. *J. Iran. Chem. Soc.* **2010**, *7*, 1−37.
(13) Evanics, F.; Diamente, P. R.; vam Veggel, F. C. J. M.; Stanisz, G. J.; Prosser, R. S. *Chem. Mater.* **2006**, *18*, 2499−2505.
(14) Sun, S.; Zeng, H.; Robinson, D. B.; Raoux, S.; Rice, P. M.; Wang, S. X.; Li, G. *J. Am. Chem. Soc.* **2003**, *126*, 273−279.
(15) Shevchenko, E. V.; Talapin, D. V.; Kotov, N. A.; O'Brien, S.; Murray, C. B. *Nature* **2006**, *439*, 55−59.
(16) Fukuoka, A.; Araki, H.; Sakamoto, Y.; Sugimoto, N.; Tsukada, H.; Kumai, Y.; Akimoto, Y.; Ichikawa, M. *Nano Lett.* **2002**, *2*, 793−795.
(17) Zhang, Y.; Yuwono, A. H.; Li, J.; Wang, J. *Microporous Mesoporous Mater.* **2008**, *110*, 242−249.
(18) Cui, F.; Hua, Z.; He, Q.; Li, J.; Guo, L.; Cui, X.; Jiang, P.; Wei, C.; Huang, W.; Bu, W.; Shi, J. *Opt. Soc. Am.* **2009**, *26*, 107−112.
(19) Klein, L. C. *Ann. Rev. Mater. Sci.* **1985**, *15*, 227−248.
(20) Berg, J. M.; Romoser, A.; Banerjee, N.; Zebda, R.; Sayes, C. M. *Nanotoxicology* **2009**, *3*, 276−283.
(21) Brydson, R. *Electron Energy Loss Spectroscopy*; Oxford: Bios in association with the Royal Microscopical Society: Great Britain, 2001.
(22) Škvarla, J. *Colloids Surf., A* **2012**, *397* (33), 1−98.